# The Response of Airfoils to Periodic Disturbances —The Unsteady Kutta Condition

D. R. Poling* and D. P. Telionis†
*Virginia Polytechnic Institute and State University, Blacksburg, Virginia*

**Two cases of unsteady flowfields over a NACA 0012 airfoil at an angle of attack are examined. The first is the classical pitching motion about the airfoil's quarter chord. The second is the flow over a fixed airfoil immersed in the wake of the pitching airfoil. Large reduced frequencies are examined. Measurements were obtained in a water tunnel by laser doppler velocimetry. Ensemble-averaged velocity measurements were obtained in the vicinity of the trailing edges of both the pitching and the fixed airfoil. The results indicate that the classical unsteady Kutta condition is clearly not valid. An extension of this condition earlier proposed by Giesing and Maskell is examined and some evidence is provided for its support.**

## I. Introduction

UNSTEADY flows about airfoils involve length scales that differ by many orders of magnitude. Solving the full Navier-Stokes equations for such problems with today's and perhaps the next generation computing machines is not practical. Methods based on interacting boundary layers will remain useful for some time to come. For unseparated flows, the trailing edge of the airfoil plays a crucial role in controlling the entire structure of the flowfield. This paper offers some experimental evidence on the physical characteristics of unsteady flow in the neighborhood of a sharp trailing edge.

Experimental work on unsteady airfoils has been reviewed carefully by McCroskey.[1,2] The specific question of whether the classical Kutta condition is violated in unsteady flows has been addressed by a number of experimentalists[3-10] as reviewed briefly by Ho and Chen.[11] With only a few exceptions, in all of these investigations it is the unsteady pressure distribution that is examined, a quantity which can offer little insight into the actual behavior of the flow in the trailing-edge region. Moreover, and perhaps more importantly, in all of these investigations no alternative condition is suggested. The fact is that for a relatively wide range of the parameters involved, the quasisteady condition is satisfied. In fact, Ho and Chen[11] point out that the range of the reduced frequencies for the validity of the steady Kutta condition is a function of the general configuration. However, situations arise in practical engineering problems where the flow departs markedly from the quasisteady behavior, as for example when blades or wings encounter gusts or when turbomachinery blades are immersed in the wake of an upstream cascade.

An extension of the Kutta condition to unsteady flow has, in fact, been suggested by Giesing[12] and Maskell.[13] Essentially, they proposed that for a changing bound circulation the stagnation streamline is an extension of the one of the two tangents to the airfoil at the sharp trailing edge. A lucid discussion of the physical arguments in favor of such a model is included in Basu and Hancock.[14] The most severe criticism of the Giesing-Maskell model centers around the fact that this unsteady condition does not reduce to the classical steady condition. As a possible explanation, Basu and Hancock[14] offer the fact that in the "unsteady problem, the curvature of the streamline emanating from the trailing edge tends to infinity as $d\Gamma/dt \to 0$" where $\Gamma$ is the bound circulation. The problem is not academic, because such situations are encountered twice within a single period of a periodic disturbance. Therefore, it is not just a limiting process for weak unsteadiness in question, but a significant phase of a dynamic phenomenon whereby the time rate of the bound circulation changes sign.

No experimental efforts have been undertaken so far to provide evidence for the validity of the Giesing-Maskell criterion. In this paper, we describe measurements of two periodic problems. The first is the classical pitching airfoil. The second is the flow over a fixed airfoil immersed in a periodic wake that represents essentially a periodic change on the angle of attack. Indeed, for the high reduced frequencies tested here, the experimental evidence supports the Giesing-Maskell criterion.

The direction of the stagnation streamline emanating from the trailing edge has been measured by Ho and Chen[11] for an airfoil in a plunging motion. They employed x wires to generate data for a streamfunction integration loop. However, they confined their attention to a single point in the period. In the present work, we use laser-Doppler velocimetry to provide data for similar integration paths. Our results pertain to a large number of phase angles covering the entire period of the oscillation as well as streamlines above and below the airfoil. Moreover, the experimental results presented here pertain to a pitching airfoil in a steady stream and a fixed airfoil in an oscillating stream.

Ho and Chen[11] took data no closer than 5% chord length downstream of the airfoil edge. They have then expressed the opinion[15] that the stagnation streamline may be turning sharply in the immediate vicinity of the sharp edge. Only such a behavior would compromise the data they obtained with the location of the airfoil edge. This is in agreement with the curvature argument presented by Basu and Hancock.[14] To shed more light on the structure of the flow in this region, we obtained measurements closer than 1% chord length to the trailing edge.

Presented as Paper 84-0050 at the AIAA 22nd Aerospace Sciences Meeting, Reno, NV, Jan. 9-12, 1984; received March 16, 1984; revision received March 1, 1985. 

*Research Associate. Department of Engineering Science and Mechanics; presently, Boeing Vertol Company, Philadelphia, PA. Member AIAA.

†Professor, Department of Engineering Science and Mechanics. Associate Fellow AIAA.

## II. The Kutta Condition

The classical Kutta condition for sharp-edge airfoils requires that, within the framework of inviscid flow theory, the stagnation streamline in the aft of the airfoil is attached to the trailing edge. This condition is sufficient to render the solution unique and, in fact, it can be easily proved that then, at least for steady flow, a number of other conditions are met at the trailing edge:

1) The pressure is continuous, or else, the loading tends to zero.

2) The velocity is finite or zero.

3) The shedding of vorticity vanishes.

4) The stagnation streamline bisects the wedge angle of the airfoil.

In fact, any of these conditions can be used to solve the problem and then all other conditions are automatically satisfied.

It has slipped the attention of many investigators that such solutions are unique only if formulated in an analytical way. If a modern panel method is used, then requiring that the rear stagnation point be located at the trailing edge is not enough to render the solution unique. There is an infinity of solutions that satisfy conditions 1, 2, and 3 and are therefore physically acceptable. All of these solutions are quite realistic if the trailing edge is somewhat rounded. In this case, the classical Kutta condition is in fact inapplicable. What is remarkable about the Kutta condition is that, in real life, a small curvature of the trailing edge does not influence the flow and the stagnation streamline leaves the airfoil in a direction that bisects the airfoil wedge. In finite panel methods for steady flows, therefore, one should also require that condition 4 is met as well.

This idea can be illustrated more clearly by virtue of the schematic representations of Fig. 1. In Fig. 1a, the classical situation of a sharp edge is depicted. Standard conformal mapping concepts convince us that the stagnation streamline bisects the wedge angle. This is simply because the image point of the wedge corner is a singularity of the transformation, the stagnation streamlines are always perpendicular to the cylinder surface, and the angles there are magnified by the same factor. The images of both angles designated by $\theta/2$ in the figure are equal to 90 deg in the transformed plane. Any real airfoil edge, of course, is not perfectly sharp. If the edge is even slightly rounded, then any direction is acceptable, as shown in Fig. 1b. Nevertheless, experimental evidence indicates that the standard analytical solution is predicting the flow with a remarkable accuracy, which implies that the trailing-edge streamline leaves the airfoil in the direction of the wedge bisector, as shown in Fig. 1c.

These arguments should not be totally reassuring. The logic is exposed to the serious question: How small should the radius of the curvature be to permit application of the classical Kutta condition? Certainly, for well-rounded trailing edges, viscous effects cannot be neglected.[16] Basu and Hancock[14] very correctly argue that there is no definite statement of the Kutta condition and each mathematical formulation "requires its own consistent Kutta condition to ensure a unique solution; the relevant and appropriate Kutta conditions needs to be formulated separately for each mathematical model."

The situation changes drastically in unsteady flow. If there is no separation upstream of the trailing edge, then the rear stagnation point coincides again with the trailing edge. However, any changes of bound vorticity require shedding of equal and opposite vorticity. Condition 2 is therefore violated. In this case, the direction of the flow in the neighborhood of the trailing edge coincides with one of the two sides of the wedge, as shown schematically in Fig. 2 and argued convincingly by Giesing[12] and Maskell.[13] The basic idea is that any stagnation streamline contained in the extended wedge corresponds to zero velocity on both sides of the airfoil; namely, for $|\phi| < \theta/2$ (Fig. 3a), $U_u = U_\ell = 0$, whereas any streamline outside the extended wedge (Fig. 3b) leads to an infinite value of the velocity on one side of the airfoil. The first case (Fig. 3a) does not allow shedding of vorticity, whereas the second (Fig. 3b) should be discarded because of the singularity. This leaves us with the situations of Fig. 2 as the only alternatives. These arguments of course would be meaningless if the interaction between the viscous and inviscid regions in the vicinity of the trailing edge is strong.

Sears[17,18] has extended the classical Howarth condition to unsteady flow. By calculating the vorticity flux shed by the boundary layers at the points of separation of a two-dimensional body, he arrived at the relationship

$$-\frac{d\Gamma}{dt} = \left[\frac{1}{2}U_e^2 - U_{sep}U_e\right]_\ell^u \tag{1}$$

where $[\ ]_\ell^u$ is the difference between the values at the upper and lower surface, respectively, $U_e$ the boundary-layer-edge velocity at separation, and $U_{sep}$ the speed of separation. In the case under consideration here, the flow stays attached until the trailing edge and therefore $U_{sep} = 0$. Equation (1) therefore readily reduces to

$$\frac{d\Gamma}{dt} = \frac{1}{2}(U_e^2 - U_u^2) \tag{2}$$

where either $U_e$ or $U_u$ is zero as depicted schematically in Fig. 2. Basu and Hancock[14] have arrived at Eq. (2) following purely inviscid arguments of vortex shedding. Moreover, they have proved that Eq. (2) is compatible with condition 1, namely that the pressure is continuous at the trailing edge.

These arguments are a natural extension of the steady flow theory and are mathematically unambiguous and consistent. However, there is a serious flaw in the logical structure described. The unsteady solutions do not tend asymptotically to the steady solution. For any time rate of change of bound circulation, no matter how small, the trailing-edge streamline forms an angle $\theta/2$ with the wedge bisector. In other words,

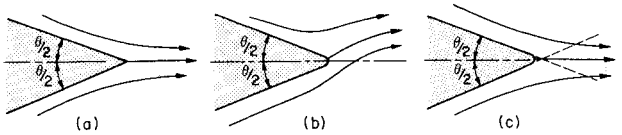


**Fig. 1 Schematic representation of trailing-edge streamlines for steady flow: a) sharp edge; b, c) rounded edge.**

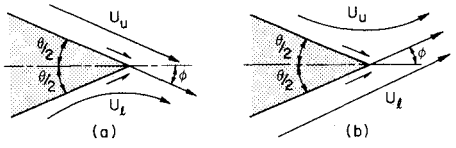


**Fig. 2 Schematic representation of trailing-edge streamlines for unsteady flow ($\phi = \theta/2$): a) for $d\Gamma/dt < 0$, shed vortices in clockwise direction; b) for $d\Gamma/dt > 0$, shed vortices in counterclockwise direction.**

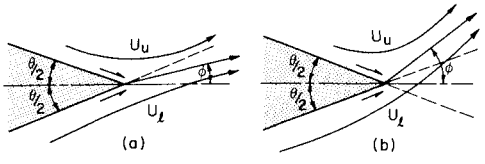


**Fig. 3 Schematic representation of trailing-edge streamlines for unsteady flow: a) if $\phi < \theta/2$, then $V_\ell = V_u = 0$; b) if $\phi > \theta/2$, then one of $V_\ell$ and $V_u$ is singular.**

$\phi$ does not tend to zero as $d\Gamma/dt$ tends to zero. What exactly happens during the time interval around the vanishing of $d\Gamma/dt$ is not well understood. Perhaps the most reliable approach is to require condition 1, namely zero loading across the trailing edge. Basu and Hancock[14] present some very encouraging numerical results using this condition. The present experimental data provide support for the Giesing-Maskell model as well as the details of how the flow changes over from the $d\Gamma/dt>0$ to the $d\Gamma/dt<0$ trailing edge flow pattern.

## III. Facilities and Equipment

Experiments were conducted in the VPI water tunnel.[19] For unsteady flows, tests in water offer significant advantages over tests in air. Realistic Reynolds numbers can be achieved in water with speeds and frequencies of unsteadiness 15 times smaller than corresponding speeds in wind tunnels. Moreover, laser-Doppler velocimetry is much more convenient in water, because it practically generates a continuous signal.

Two NACA 0012 airfoils with a 4 in. (101.6 mm) chord were mounted in the test section as shown in Fig. 4. The first airfoil was connected to a four-bar linkage system that facilitated pitching about its quarter chord. The frequency of oscillations was controlled by an electronic feedback system to within 1% of the set value. The mechanism permits continuous adjustment of the amplitude of oscillation. This airfoil was also used to generate a disturbance field for the second airfoil that was mounted two chord lengths downstream (see Fig. 4). The wake of the pitching airfoil was calibrated and data were obtained in the immediate vicinity of its trailing edge. The measuring grid shown in Fig. 4 was separated in five groups designated with Roman numerals. Groups I and II were employed for contour integrations and the determination of instantaneous streamlines in the neighborhood of the trailing edges of the leading and trailing airfoils, respectively. Groups III and IV were used to track the vortices upstream and over the trailing airfoil, respectively, and group V was used to provide a crude picture of the mean and fluctuating velocity field in the wake of the leading airfoil.

To eliminate the end effects, a special test section was designed and constructed. The main idea was to provide a set of false inner side walls and allow the wall boundary layers to be directed behind the false walls. To control the amount of flow through the narrow passages and avoid separation at the leading edges of the walls, a set of flaps were mounted at their trailing edges. An alternate method consists of a section system, which was designed and constructed. Only the first method has been tested thus far. The mean boundary-layer velocity and rms of the fluctuation profiles were measured on both sides of the false walls. This proved that the thickness of the side wall boundary layers is less than 2.5% of the airfoil span.

In a backward-scattering mode, the sending and receiving optical paths of laser-Doppler velocimetry (LDV) are identical, permitting traversing by mirrors. A traversing mechanism with two mirrors was recently designed, constructed, and tested. The system is shown schematically in Fig. 5. Two stepping motors control the motion in two directions. A laboratory computer (MINC-11) is interphased with the stepping motors. The path of the measuring volume can thus be programmed in advance. The laboratory computer was later interphased directly with the LDV counter. The computer was thus employed to control the shape and size of the contours traversed by the measuring volume, obtain ensemble averages, and store the data. Data were also obtained by a two-channel fast Fourier transform (FFT) signal analyzer (HP 5420). Ensemble averages of waveforms of the signal were obtained and stored in this way.

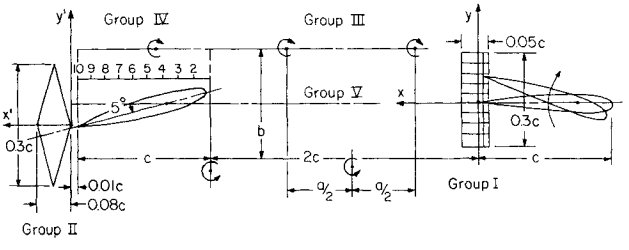


**Fig. 4 Schematic representation of the experimental arrangement. The flow is from right to left. General grid layout shows the five groups of measuring points (length measured in hundredths of chord c).**

## IV. The Pitching Airfoil and Its Wake

Careful experiments were conducted in the neighborhood of the trailing edge of the pitching airfoil. The freestream velocity was $U_\infty = 20$ cm/s and the pitching frequency was equal to $f = 1.5$ Hz. These correspond to a Reynolds number and a reduced frequency $Re = U_\infty c/\nu = 20{,}000$ and $k = \pi fc/U_\infty = 2.4$, respectively. The amplitude of oscillation (peak to peak) was $\Delta\alpha = 20$ deg. A bank of conditionally averaged data were obtained for the points of group I along four vertical lines. This mesh was chosen in such a way that contour integrations of the quantity

$$\psi = \int (u\,dy - v\,dx) \tag{3}$$

along the upper of lower paths could be obtained in order to determine the direction of streamlines in the immediate neighborhood of the edge. In this way, data could be obtained for five azimuthal edge positions, namely the positions $x_1 = 0$, $y_1 = 3$ and $x_2 = -1$, $y_2 = 9$ where all coordinates are measured in terms of a hundredth of the chord length. The above positions correspond to angles of attack of $\alpha_1 = 2.25$ deg and $\alpha_2 = 6.82$ deg, respectively. The horizontal velocity component was measured along the vertical sides and the vertical component was measured along the top and bottom sides of a rectangular contour, respectively. The data mesh was chosen in such a way that the path of the trailing edge due to pitching oscillations about the quarter-chord permits contour integration for trailing-edge positions corresponding to $x_1 = 0$, $y_1 = 0$; $x_2 = 0$, $y_2 = 3$; $x_3 = -1$, $y_3 = 9$; $x_4 = 0$, $y_4 = -3$; and $x_5 = -1$, $y_5 = -9$ and perhaps with some errors positions $x = -2$ and $y = \pm 12$.

In each case, 50-70 conditional averages were obtained. A trigger was supplied externally by the oscillating mechanism. About two periods of the conditional averaged response were obtained for each point on the data mesh. It was thus possible to perform the integration of Eq. (3) by collecting all the

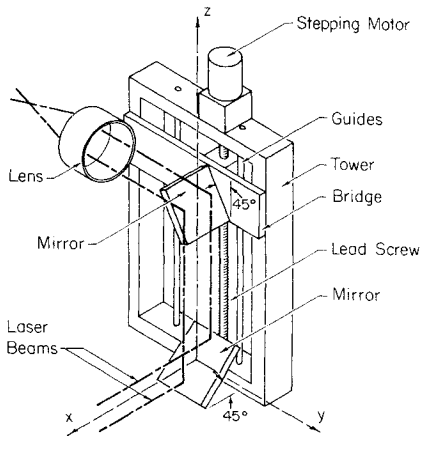


**Fig. 5 Traversing mechanism for LDV measurements.**

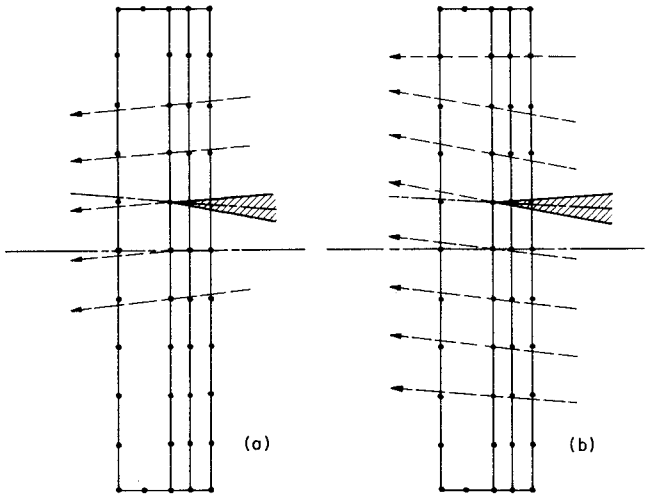


Fig. 6 Instantaneous trailing-edge streamlines at the instant when $\alpha = 2.25$ deg, which corresponds to the trailing edge at position $x = 0$, $y = 3$: a) upstroke; b) downstroke (lengths measured in hundredths of c).

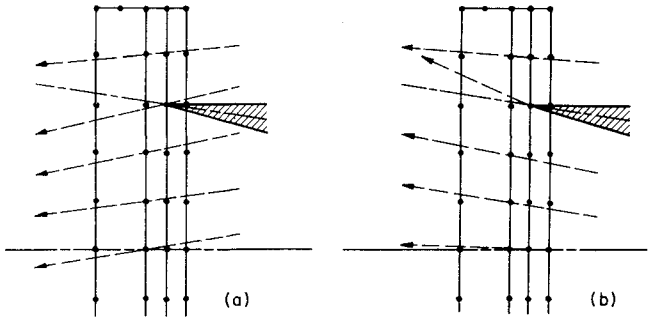


Fig. 7 Instantaneous trailing-edge streamlines at the instant when $\alpha = 6.82$ deg, which corresponds to the trailing edge at position $x = -1$, $y = 9$: a) upstroke; b) downstroke (lengths measured in hundredths of c).

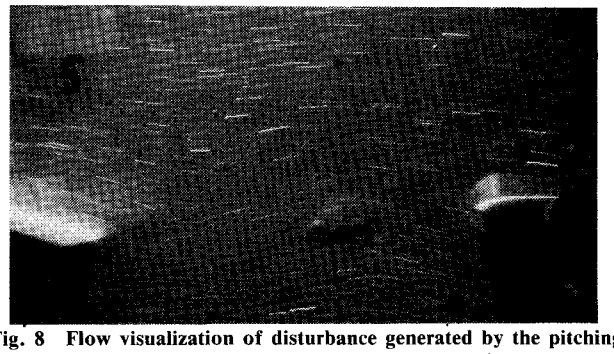

Fig. 8 Flow visualization of disturbance generated by the pitching airfoil (the direction of the flow is from left to right).

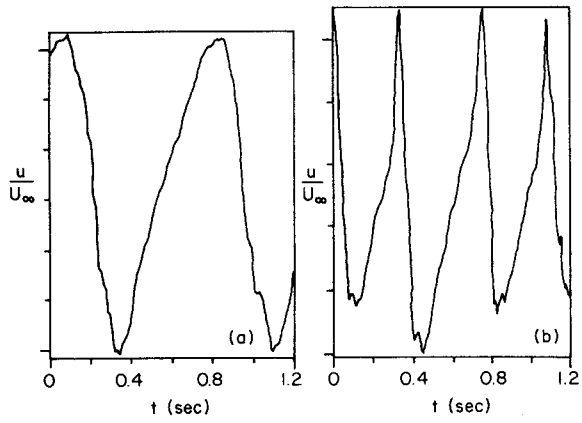


Fig. 9 Averaged time record of velocity fluctuations (vertical scale arbitrary): a) trailing edge at position $x = 25$, $y = 18$; b) at position $x = 25$, $y = 0$ (lengths measured in hundredths of c).

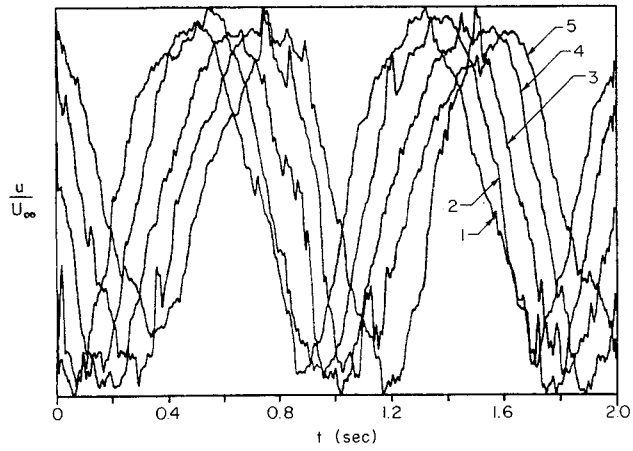


Fig. 10 Velocity waveforms obtained at grid points of group IV (see Fig. 4) over the fixed airfoil (vertical scale arbitrary).

velocities in space at a particular phase. The two paths of integration as suggested by Ho and Chen,[11] namely along the upper and lower branches resulted in a discrepancy of about 10%. However, it is interesting that this discrepancy is consistent. This could be attributed to the boundary layers that follow the blade in its motion as it cuts through the mesh. In all cases, we took the average of the two results, which essentially bridged the consistent gap.

In order to gain more confidence in these results, contour integrations were also performed starting at points higher and lower then the instantaneous location of the trailing edge. Examples of such data are plotted in Figs. 6 and 7. The slopes of all streamlines in the neighborhood of the trailing edge are practically equal. For a reduced frequency of 2.4, therefore, it appears that the trailing-edge streamline is approximately tangent to the wedge formed at the trailing edge, in accordance with the Giesing-Maskell model. It should be added that the results presented are calculated in a frame of reference fixed on the airfoil. It is in this frame that the Giesing-Maskell pattern should be observable. The necessary correction to account for rotating coordinates was calculated analytically, because it involves terms like $\int \omega r \cos\theta dy$ and $\int \omega r \sin\theta dx$, where $\omega, r$, and $\theta$ are the angular velocity, polar radius, and polar angle, respectively. Since $r\cos\theta$ and $r\sin\theta$ are equal to $y$ and $x$, respectively, these integrals can be easily evaluated. In this way, we were able to generate segments of instantaneous streamlines in the immediate neighborhood of the trailing edge.

The wake of the pitching airfoil was studied visually using a technique developed in our laboratory.[19] The flow visualization of Fig. 8 displays a wavy pattern of particle paths that are nearly parallel to the instantaneous velocity vectors. This pattern is due to the vortices shed periodically by the trailing edge of the pitching airfoil. However, recirculating flow patterns can be detected only in frames that move with the vortices. Some crude data were then obtained in the downstream region of the oscillating airfoil in order to document the properties of the flow that the second airfoil encounters. The variation of the mean velocity and the amplitude of the velocity fluctuation respectively were recorded[20] at three stations downstream of the oscillating airfoil. As expected, the pitching of the airfoil generates in the mean a region of accelerated flow. The mean velocity along the centerline of the airfoil is about 20% larger than the velocity away from the airfoil.

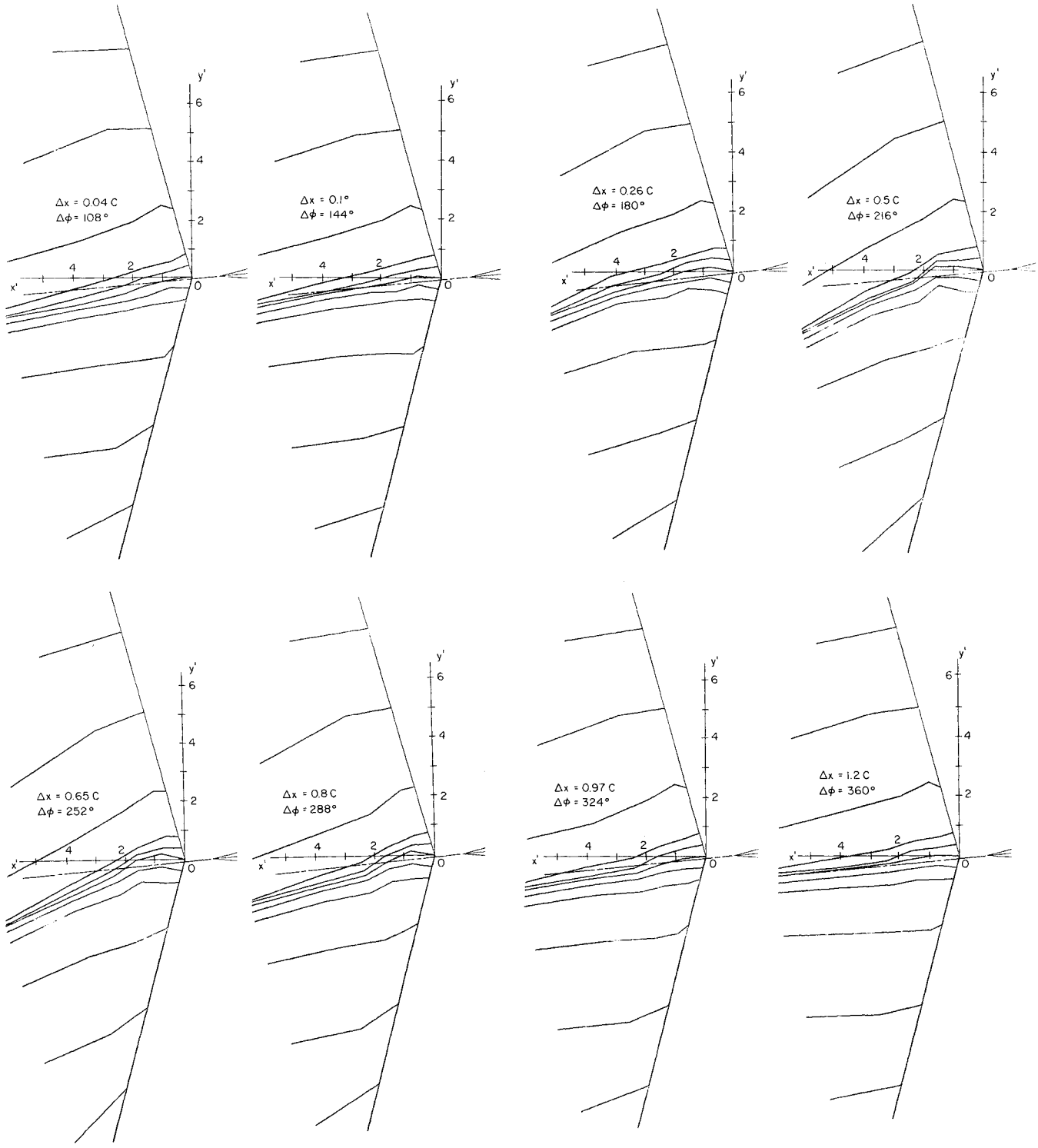


**Fig. 11 Instantaneous streamlines in the neighborhood of the trailing edge of the fixed airfoil as obtained by conditional averaging of the LDV signals. The quantity is the distance of the instantaneous position of a drifting vortex on the upper side of the fixed airfoil, measured from its leading edge; $\Delta\phi$ is the corresponding phase angle of the period.**

Averaged wave patterns of the velocity response are shown in Fig. 9 for two points, one away from the axis of the airfoil and one along the $x$ axis. As anticipated, at a point away from the axis, the velocity oscillates with the frequency of the imposed fluctuation. On the axis, the velocity is strongly affected by the passage of the trailing edge and displays a frequency twice as large as the driving frequency. What appears to be interesting is that at points not far from the axis (not shown here) both frequencies can be detected. A more detailed study of the flow in this region can be found in Refs. 20 and 21.

## V. Tracking of Vortices

To track the position and the path of the vortices shed by the pitching airfoil measurements were obtained along a number of grid points designated by III and IV in Fig. 4. At all points the $u$ component of the velocity was measured and conditionally averaged. For points positioned above the vortex street, a maximum in the waveform indicates the instant that a vortex with positive vorticity is immediately below. Similarly, a minimum indicates the instant that a vortex with negative vorticity is immediately below the point of measurement. Measuring the time elapsed between two

maxima $t_0$ at two different points spaced a distance $x_0$ apart gives the vortex drift velocity $x_0/t_0$. Moreover, the time between two consecutive peaks in the signal from a point in space gives the period $T$ that then provides the spacing of the vortices, $a = x_0 T/t_0$ (see Fig. 4).

We then assumed that the velocity field induced by the vortices is approximately equal to the field generated by an infinite array of vortices with the same spacing. This configuration accepts a closed-form solution,[22] which can be recast in terms of $u_{max}$ and $u_{min}$ measured at a height $c/2$ from the axis of the system of vortices,

$$\frac{a}{T} = U_\infty + \frac{\Gamma}{2a}\coth\frac{\pi b}{a} \tag{4}$$

$$u_{max} = \frac{\Gamma}{2a}\left[\coth\frac{\pi}{2a}(c-b) + \tanh\frac{\pi}{2a}(c+b)\right] \tag{5}$$

$$u_{min} = \frac{\Gamma}{2a}\left[\coth\frac{\pi}{2a}(c+b) + \tanh\frac{\pi}{2a}(c-b)\right] \tag{6}$$

where $\Gamma$ is the strength of the vortices and $T$ the period. This system can be solved for $a$, $b$, and $\Gamma$ if the quantities $T$, $u_{max}$, and $u_{min}$ are known. In the present case, we measured $a$ as well and then calculated the quantities $b$ and $\Gamma$. We found $a = 0.95c$, $\Gamma = 0.4\ CU_\infty$. A re-evaluation of this approximation and a more elaborate computation scheme can be found in Ref. 21.

Data obtained at grid points IV resulted in waveforms that allow us to measure the propagation of the oncoming vortices. An example of a few velocity waveforms are displayed in Fig. 10. The time delay from peak to peak corresponds to the time required for the vortex to drift from one point to the next.

## VI. The Fixed Airfoil and Its Wake

Measurements in the neighborhood of the trailing edge of the fixed airfoil were conducted about a year later than measurements around the pitching airfoil. It was then decided to define an alternative shape of the measurement grid and the integration contours. Diamond shape contours were chosen as shown in Fig. 4. The advantage of this choice is that the velocity components required for integration of Eq. (3) do not deviate much from the local direction of the velocity.

The measurements obtained in this way for $U_\infty = 10$ cm/s, $f = 1.2$ Hz, $Re = 10{,}000$, $k = 3.9$ are displayed in Fig. 11. In the same figure, we show the relative position of oncoming vortices as determined by tracking of vortices (see Sec. V). Apparently, the streamline structure in the immediate neighborhood of the trailing edge is deviating drastically from the preferred direction of the flow around it. The thickness of the boundary layer was found to be approximately equal to $2c/100$ and therefore the region immediately downstream of the trailing edge is totally immersed in the viscous layers. The fact that, within a distance of $3c/100$-$5c/100$ from the trailing edge, the streamline patterns display large curvatures is very significant. It implies that there are strong cross-flow pressure gradients. In other words, this is clearly a region of strong viscous-inviscid interaction just like in the case of steady flow over a rounded trailing edge. The pressure variation across the free-shear layer is not negligible. The pressure jump coefficient was estimated to be 10% of the mean pressure coefficient over the airfoil.

In the framework of the theory of inner and outer expansions, our experimental evidence implies that in the inviscid outer solution a jump in the pressure could be acceptable at the trailing edge. Thus, the condition of zero loading is inapplicable in high-frequency unsteady flows.

The fact that the streamlines in the viscous shear layer align themselves with the inviscid flow at a radial distance of $3c/100$-$5c/100$ from the trailing edge indicates that the pressure discontinuity across the trailing-edge vortex sheet is eliminated quickly.

It remains for the numerical analysts to investigate whether imposing the zero loading condition at the trailing edge or a few hundredths of a chord length downstream makes a significant difference for global properties like lift and pitching moment. We propose that an alternative condition may be to impose zero loading at an imaginary extension of the airfoil. Outside the truly viscous region, the potential flow appears to follow again approximately the Giesing-Maskell criterion, although at some instances the flow appears to form angles $\phi > \theta/2$, as depicted schematically in Fig. 3b.

Following the advice of one of the reviewers, we have recently obtained dye visualizations that indicate that the continuous vortex sheets emanating from the trailing edge of the leading airfoil have not yet rolled up into nearly discrete vortices when they interact with the trailing airfoil. The discrepancies noted above whereby $\phi$ appears even greater than $\theta/2$ may be due to concentrated vorticity washing over the airfoil and perhaps interacting with the attached boundary layers. Detailed boundary-layer measurements indicate that perhaps due to such disturbances, the boundary layers near the edge of the trailing airfoil are turbulent.

## VII. Conclusions

The only case of airfoil flows that can be conveniently and unambiguously treated with inviscid theories is the case of a cusped trailing edge. For finite-angle trailing edges, the classical solution of steady potential flow equations is unique, if the stagnation point is positioned at the edge. For inviscid flows then, the trailing stagnation streamline is tangent to the bisector of the wedge at the trailing edge. Following the majority of the contemporary authors, we say that flows with such characteristics satisfy the "classical Kutta condition."

The present experimental data indicate that, for periodic flows with reduced frequencies larger than $\omega c/2U_\infty = 2$ and not very small amplitudes, the classical Kutta condition is never satisfied. The reduced frequency has been usually employed as a parameter controlling the extent of the validity of the Kutta condition. It is proposed here that a more meaningful parameter should be the relative acceleration of the trailing edge for a pitching airfoil or the time rate of change of the velocity difference above and below the trailing edge for a fixed airfoil. An equivalent but universal criterion is the reduced time rate of change of the bound circulation, namely the dimensionless quantity $(d\Gamma/dt)_{max}/U_\infty$ where $\Delta\Gamma$ is the amplitude of circulation.

An alternative condition, equivalent to the classical Kutta condition, is the condition of zero loading at the trailing edge. What appears at first to be an obvious requirement soon turns out to be an ambiguous condition. For an inviscid theory, there can be no pressure jump across two neighboring streamlines, unless a solid body is interfering. Within the approximation of this theory, boundary layers are infinitely thin vortex sheets and free vortex sheets cannot sustain forces. In other words, the edge cannot be loaded. All of these arguments are valid, if the interaction between the viscous and inviscid regions is weak.

In both cases considered here, which correspond to reduced frequencies of $k = 2.4$ and $K = 3.9$ for the pitching and fixed airfoils, respectively, the classical Kutta condition is clearly violated. The second case provides data on a much finer measuring grid that penetrates the viscous region. In this region, there is ample evidence of finite normal pressure gradients and therefore nonzero trailing-edge loadings. However, outside the viscous regions, it appears that for both cases the Giesing-Maskell criterion approximately holds, as long as $d\Gamma/dt$ is far from its zero. During time intervals

centered about the zero of $d\Gamma/dt$, the trailing-edge streamline changes direction smoothly with time.

The measurements of the second problem discussed here extend well within the viscous region and reveal the true character of the flow in the vicinity of the trailing edge. They also indicate that the violation of the condition of zero loading does not extend further than 3% of the chord length downstream of the trailing edge. It remains for the numerical analyst to examine the influence of imposing zero loading at the trailing edge or a short distance downstream. Still, this may not be an appropriate remedy, because for unsteady flow the loading near the trailing edge varies very sharply with the distance from the trailing edge. Even a few percent of the chord length may have a significant effect on global characteristics like instantaneous or averaged lift and drag.

## Acknowledgment

This research was supported by NASA, Project 47-004-801. The monitors of this grant, Dr. E. C. Yates and later Dr. W. J. McCroskey, have contributed substantially by their support and criticism. Drs. L. W. Carr and W. J. McAlister of NASA Ames have also made many helpful suggestions.

## References

[1]McCroskey, W. J., "Some Current Research in Unsteady Fluid Dynamics—The 1976 Freeman Scholar Lecture," *Journal of Fluids Engineering,* Vol. 224A, 1954, pp. 1-23.

[2]McCroskey, W. J., "Unsteady Airfoils," *Annual Review of Fluid Mechanics,* Vol. 14, 1982, pp. 285-311.

[3]Kovasznay, L. S. G. and Fujita, H., "Unsteady Boundary Layer and Wake Near the Trailing Edge of a Flat Plate," *Proceedings of IUTAM Symposium,* Recent Research on Unsteady Boundary Layers, E. A. Eichelbrenner, ed., Les Presses de l'Université Laval, Quebec, Canada, 1972, pp. 805-833.

[4]Achibald, F. S., "Unsteady Kutta Condition at High Values of the Reduced Frequency Parameter," *Journal of Aircraft,* Vol. 12, 1975, pp. 545-550.

[5]Ostdiek, F. R., "A Cascade in Unsteady Flow," *Unsteady Phenomena in Turbomachinery,* AGARD CP 177, 1975, pp. 26-1-26-13.

[6]Commerford, G. L. and Carta, F. O., "Unsteady Aerodynamic Response of a Two Dimensional Airfoil at High Reduced Frequency," *AIAA Journal,* Vol. 12, 1974, pp. 43-48.

[7]Satyanarayana, B. and Davis, S., "Experimental Studies of Unsteady Trailing Edge Conditions," *AIAA Journal,* Vol. 16, Feb. 1978, pp. 125-129.

[8]Bechert, D. and Pfizenmaier, E., "Optical Compensation Measurements on the Unsteady Exit Condition at a Nozzle Discharge Edge," *Journal of Fluid Mechanics,* Vol. 71, 1975, p. 123.

[9]Fletter, S., "Trailing Edge Conditions for Unsteady Flows at High Reduced Frequency," AIAA Paper 79-0152, 1979.

[10]Ho, C.-M. and Chen, S. H., "Unsteady Wake of a Plunging Airfoil," AIAA Paper 80-1446, 1980.

[11]Ho, C.-M. and Chen, S. H., "Unsteady Kutta Condition of a Plunging Airfoil," *Unsteady Turbulent Shear Flows,* R. Michel, J. Cousteix and R. Houdeville, eds., Springer, Berlin, May 1981, pp. 197-206.

[12]Giesing, J. P., "Vorticity and Kutta Condition for Unsteady Multi-Energy Flow," *Transactions of ASME, Journal of Applied Mechanics,* Vol. 36, 1969, pp. 608-613.

[13]Maskell, E. C., "On the Kutta-Joukowski Condition in Two-Dimensional Unsteady Flow," Unpublished note, Royal Aircraft Establishment, Farnborough, England, 1971.

[14]Basu, B. C. and Hancock, G. J., "The Unsteady Motion of a Two-Dimensional Aerofoil in Incompressible Inviscid Flow," *Journal of Fluid Mechanics,* Vol. 87, 1978, pp. 159-178.

[15]Ho, C.-M., University of Southern California, Los Angeles, CA, private communication, 1982.

[16]Vatsa, V. N., Werle, M. J., and Verdon, J. M., "Viscid/Inviscid Interaction at Laminar and Turbulent Symmetric Trailing Edges," AIAA Paper 82-0165, 1982.

[17]Sears, W. R., "Some Recent Developments in Airfoil Theory," *Journal of the Aeronautical Sciences,* Vol. 23, No. 5, 1956, pp. 490-499.

[18]Sears, W. R., "Unsteady Motion of Airfoils with Boundary-Layer Separation," *AIAA Journal,* Vol. 14, Feb. 1976, pp. 216-220.

[19]Koromilas, C. A. and Telionis, D. P., "Unsteady Laminar Separation: An Experimental Study," *Journal of Fluid Mechanics,* Vol. 97, 1980, pp. 347-384.

[20]Poling, D., "Airfoil Response to Periodic Disturbances—The Unsteady Kutta Condition," Ph.D. Dissertation, Virginia Polytechnic Institute and State University, Blacksburg, Aug. 1985.

[21]Mathioulakis, D. S., Kim, M. J., Telionis, D. P., and Mook, D. T., "The Near Wake of a Pitching Airfoil," AIAA Paper 85-1621.

[22]Milne-Thomson, L. M., *Theoretical Hydrodynamics,* The Macmillan Company, 4th ed. 1960.